

Article

Machine Learning Composite-Nanoparticle-Enriched Lubricant Oil Development for Improved Frictional Performance—An Experiment

Ali Usman ^{1,2,*} , Saad Arif ³ , Ahmed Hassan Raja ⁴, Reijo Kouhia ¹, Andreas Almqvist ⁵ 
and Marcus Liwicki ² 

¹ Structural Engineering, Faculty of Built Environment, Tampere University, 33720 Tampere, Finland

² Department of Computer Science, Electrical and Space Engineering, EISLab, Division of Machine Learning, Luleå University of Technology, 97187 Luleå, Sweden

³ Department of Mechanical Engineering, HITEC University, Taxila 47080, Pakistan

⁴ Department of Mechanical Engineering, COMSATS University Islamabad, Wah Cantt. 47040, Pakistan

⁵ Department of Engineering Sciences and Mathematics, Division of Machine Elements, Luleå University of Technology, 97187 Luleå, Sweden

* Correspondence: ali.usman@ltu.se

Abstract: Improving the frictional response of a functional surface interface has been a significant research concern. During the last couple of decades, lubricant oils have been enriched with several additives to obtain formulations that can meet the requirements of different lubricating regimes from boundary to full-film hydrodynamic lubrication. The possibility to improve the tribological performance of lubricating oils using various types of nanoparticles has been investigated. In this study, we proposed a data-driven approach that utilizes machine learning (ML) techniques to optimize the composition of a hybrid oil by adding ceramic and carbon-based nanoparticles in varying concentrations to the base oil. Supervised-learning-based regression methods including support vector machines, random forest trees, and artificial neural network (ANN) models are developed to capture the inherent non-linear behavior of the nano lubricants. The ANN hyperparameters were fine-tuned with Bayesian optimization. The regression performance is evaluated with multiple assessment metrics such as the root mean square error (RMSE), mean squared error (MSE), mean absolute error (MAE), and coefficient of determination (R^2). The ANN showed the best prediction performance among all ML models, with 2.22×10^{-3} RMSE, 4.92×10^{-6} MSE, 2.1×10^{-3} MAE, and 0.99 R^2 . The computational models' performance curves for the different nanoparticles and how the composition affects the interface were investigated. The results show that the composition of the optimized hybrid oil was highly dependent on the lubrication regime and that the coefficient of friction was significantly reduced when optimal concentrations of ceramic and carbon-based nanoparticles are added to the base oil. The proposed research work has potential applications in designing hybrid nano lubricants to achieve optimized tribological performance in changing lubrication regimes.

Keywords: machine learning; friction; lubrication; nanoparticles; tribology; artificial neural network; Bayesian optimization



Citation: Usman, A.; Arif, S.; Raja, A.H.; Kouhia, R.; Almqvist, A.; Liwicki, M. Machine Learning Composite-Nanoparticle-Enriched Lubricant Oil Development for Improved Frictional Performance—An Experiment.

Lubricants **2023**, *11*, 254.

<https://doi.org/10.3390/lubricants11060254>

Received: 27 April 2023

Revised: 4 June 2023

Accepted: 6 June 2023

Published: 9 June 2023



Copyright: © 2023 by the authors. Licensee MDPI, Basel, Switzerland. This article is an open access article distributed under the terms and conditions of the Creative Commons Attribution (CC BY) license (<https://creativecommons.org/licenses/by/4.0/>).

1. Introduction

Metal-on-metal interfaces are found abundantly in engineering applications. Some examples are mechanical seals, bearings, pistons/plungers, and gears. These interfaces are prone to wear for various loading conditions. For instance, an intuitive mapping of the wear mechanism of metallic and non-metallic materials with lubricating conditions was graphically presented by Lim et al. [1]. A lubricant may be utilized to establish a thin lubricating film to separate the interfacial surfaces and reduce friction and wear.

However, the lubricating film developed by traditional and non-traditional lubricants may not be sustained during operation due to the high loads and relative speed of the mating surfaces [2,3]. Recent advances in nanoparticle (NP)-based lubricant additives have shown promising results in reducing the coefficient of friction (CoF) and wear of highly loaded interfaces operating in the boundary lubrication regime and increasing the load-carrying capacity of full-film hydrodynamic lubricated interfaces. Single-NP-based lubricant oil blends have been evaluated extensively for the last two decades. However, optimizing oil blends for more than one additive particle is needed to address the varying demands of the tribo-pairs for varying lubricating domains.

Several studies have investigated the use of NP as lubricant additives to improve the antiwear and frictional performance of lubricating oils. For example, CuO/Al₂O₃ [4] and Bi₂O₃ [5] NPs were found to reduce friction and wear scar diameter (WSD), whereas CeO₂ was shown to facilitate the frictional performance of polyamide-imide/polytetrafluoroethylene lubricating coatings [6] and engine oils [7]. When used in combination with ZDDP, CeO₂ NP was found to improve antiwear performance even further [8]. Cu [9] and CuO [10], and TiO₂ [11] NPs were also found to improve the thermal conductivity and rheological properties of lubricating oils, respectively. The addition of SiO₂ NP was reported to increase the load-carrying capacity of soya bean and sunflower oil [12], whereas the addition of CuO NP to coconut oil resulted in the lowest friction and a polishing effect on worn surfaces [13].

Mirzaamiri et al. [14] introduced nanodiamonds to water, resulting in a 70% reduction in friction and an 88% reduction in wear that was attributed to the ball-bearing effect of the nanodiamond. Wu et al. [15] added sulfonated graphene to water, increasing viscosity by 25.8% and reducing the WSD and CoF by 74% and 15.7%, respectively. Xu et al. [16] studied the effect of graphene nanosheet (GNS) and Ag hybrids on phenolic composites, reporting that a 9 wt% GNS/Ag hybrid reduced the friction coefficient and wear rate by 40% and 72%, respectively, due to strong molecular interactions. Wang et al. [17] found that thicker copper coated with molybdenum disulfide had a lower friction coefficient but exhibited more severe wear. Yu et al. [18] reported that hydrated silica tribofilm reduced the CoF of MoAlB ceramic to 0.12. Pham et al. [19] showed that SiO₂ enhances the anti-oxidation of lubricants. Simonovic et al. [20] found that the wear of WSC-coated ceramic is reduced under low loads and more WS₂ monolayers are present; however, abrasive wear occurs at loads above 8 N. Xu et al. [21] investigated materials containing 1% kyanite with the best braking performance. Chen et al. [22] compared Si₃N₄-based and carbon-rich MLG-based MLG/Si₃N₄ ceramics and found that the combination of MLG and Si₃N₄ improved wear resistance and reduced the CoF. Fahad et al. [23] studied base oil containing modified TiO₂/CuO NPs, which improved the viscosity index and load-carrying capacity. Sharma et al. [24] found that mixing alumina/graphene (GnP) hybrid NPs reduced cutting tool wear and nodal temperature. Huang et al. [25] found that GO–Al₂O₃ hybrid NPs provided better friction and wear performance than pure GO or Al₂O₃ due to the GO layer preventing surface asperities from direct contact and the Al₂O₃ tribo-layer acting as a load bearer to polish asperities.

Besides ceramic and carbon-based NPs, various studies [26–28] have also investigated the tribological performance of ferrous-NP-based lubricants. Oliveira et al. [26] additized PAO 8 oil with Fe₂O₃ NP to evaluate the lubricant performance for reduced friction and wear. The boundary lubrication resulted in increased scuffing resistance and reduced wear rates by up to 27% for high loads due to the intrinsic properties of metallic oxides. Another study [27] investigated the effect of coated magnetic NPs dispersed in trimethylolpropane trioleate base oil. The Nd and Fe₃O₄ NPs in 0.015 wt% concentration significantly reduced the CoF and WSD by 29% and 67%, respectively, in comparison with the base oil. Alvi et al. [28] enhanced the tribological performance of drilling fluids with iron oxide-based NP. Fe₂O₃ NP in a 0.019 wt% concentration reduced the CoF by 47% and 45% with dispersion in bentonite and KCl-based base fluids, respectively. This indicates that hybrid lubricant blends can outperform previously formulated lubricants; however, application-

and operating-condition-dependent optimization is needed. It is a delicate task involving many independent parameters and requiring a highly robust optimization scheme.

Machine learning (ML)-based methodology has shown the capability to handle many multi-featured input parameters and target the desired outcome with high accuracy and precision. Bhaumik et al. [29] presented a method for designing multiple NP-based bio-lubricants using a multi-layered artificial neural network (ANN). The ANN-based model was optimized with a genetic algorithm and the additized biolubricant showed a decrease in the CoF of 45–50% compared with mineral oils. Humelnicu et al. [30] used a feed-forward ANN to obtain the minimum CoF for blended diesel fuel by optimizing the concentrations of two vegetable oils. A CoF of 0.00156 was achieved using 4% sunflower oil, based on the results from the ANN computations. Halder et al. [31] designed an ANN-based regression estimator to predict the dynamic viscosity of multi-walled carbon nanotubes (MWCNT) and SiO₂-based nano lubricant in a 20:80 ratio. The perfect estimation was found within a 2.62% maximum deviation by comparing experimental data with the model predictions. Recently, Esfe et al. [32] used a quasi-Newton algorithm based on a multi-layered ANN to predict the viscosity of a hybrid nano lubricant with high precision. The trained Levenberg–Marquardt (LM)-based regression learner achieved a mean squared error (MSE) of 6.15×10^{-4} while estimating the observed behavior of a hybrid lubricant blend of SAE40 oil additized with MWCNT and Al₂O₃ at a 10:90 concentration ratio. Table 1 summarizes studies that effectively employed ML-based data-driven approaches to model the inherent non-linearities of nano lubricants.

Table 1. List of similar studies on ML-based approaches for tribological performance prediction.

Ref.	Methodology	Input/Output Parameter	Base Oil/Additive	Performance
[29]	ANN, GA	Load, speed, concentration/ CoF	NCO, CMO/ GRT, MWCNT, GRPHN, ZnO	CoF ↓ by 45–50% WSD ↓ by 87.5%
[30]	FF-ANN	Concentration/ CoF	Regular diesel fuel/ Sunflower oil, Rapeseed oil	CoF: 1.56×10^{-3} with 4% sunflower oil
[31]	ANN	Temperature, volume fraction, shear rate/Viscosity prediction	SAE68 hydraulic oil/ MWCNT, SiO ₂	R ² : 0.998 RMSE: 2.135415
[32]	LM-based MLP	Temperature, volume fraction, shear rate/Viscosity prediction	SAE40/ MWCNT, Al ₂ O ₃	R: 0.9999 MSE: 6.15×10^{-4} −2% < MOD < 2%
[33]	DT, RF, GLM, ANN	Temperature, volume fraction/ Kinematic viscosity prediction	SAE30, Hydrex100, EP90/ Al ₂ O ₃ , CeO ₂	R ² : 0.861 (SAE30) R ² : 0.971 (Hydrex100) R ² : 0.973 (EP90)
[34]	LM-ANN	Temperature, volume fraction, shear rate/Viscosity prediction	SAE50/ MWCNT, Al ₂ O ₃	MSE: 3.58 R: 0.999

GA: genetic algorithm; NCO: neat castor oil; CMO: commercial mineral oil; GRT: graphite; GRPHN: graphene; FF: feed-forward; MLP: multi-layer perceptron; MOD: margin of deviation; DT: decision trees; RF: random forest; GLM: generalized linear model; ↓ shows a decrease.

The studies reviewed above show that NP enrichment can be used to control the dynamic and static properties of the lubricant. However, the mechanisms that govern the changes in lubrication performance are complex and not yet fully understood. Moreover, there exist many parameters that affect the outcome of NP addition to the base lubricant. Due to the complexity of the mechanism and the numerous design parameters of hybrid lubricant blends containing multiple NPs, there is a gap in the literature presenting studies on the possibilities of obtaining performance improvements. In this work, random forest trees (RFT) and support vector machines (SVM)-based regression models are initially developed to capture the NP-based lubricant behavior. In the final approach of designing computational methods, multi-layered ANNs are developed and trained to predict the performance of multiple-NP-based lubricants and their hybrids to minimize the CoF. The

details of the experiments, training dataset, modeling, and results are discussed and the capabilities of the ML-based techniques are compared. The CoF is analyzed for varying operating conditions and the evolution of lubricating regimes is analyzed for individual and hybrid oils. Optimization of the NP concentrations for varying lubricating regimes is also evaluated.

2. Design of Experiment

The experimental dataset was created using a pin-on-disc tribometer for experiments with different NP-based lubricants as shown in Figure 1. A commercially available oil, 5W30 by Shell plc, was used in this study to create NP-based blends, and a comparison is drawn with the same oil without NP. The experiments were carried out with varying values of the parameters involved. The parameters under consideration were the NP concentrations in weight percentages (wt%) for silicon dioxide (SiO_2) and nano graphite (NG) with varying load (Newton, N) and speed (revolutions per minute, RPM). The single output CoF was recorded for each experiment. The experiments were conducted at two load levels and five speed levels for all the lubricants comprising the plain oil (PO) without NP and PO with both NPs individually. For each NP, two levels of concentration, along with the above load and speed levels, are used because the load and speed both influence the lubrication regime. Similarly, the NP concentration affects the oil viscosity, which in turn is an important parameter controlling the lubricating regime experienced by the tribo-pair. Therefore, five factors and the corresponding three levels have been adopted to explore the pure hydrodynamic, mixed, and boundary lubrication of the tribo-interface for varying design parameters and to explore the effect of the combination of NPs on the said lubricating regimes.

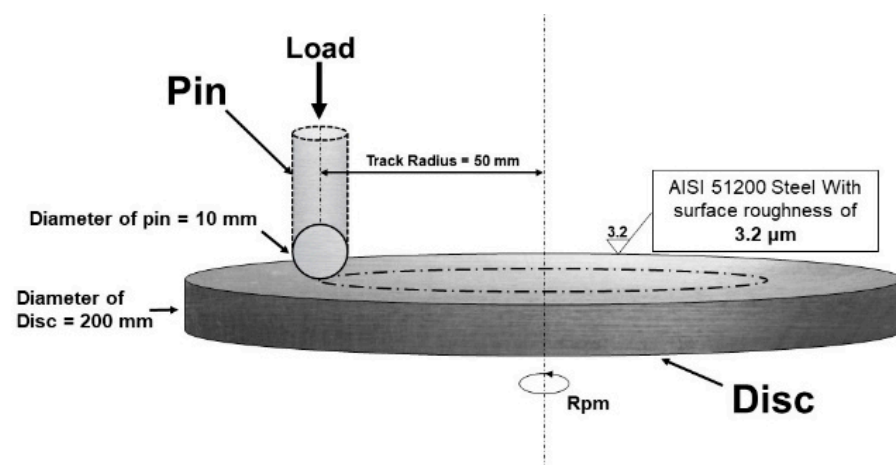


Figure 1. Pin-on-disc schematic illustrating surface parameters, geometry, and loading conditions.

The dataset array was generated for 30 experiments (number of samples) according to the values shown in Table 2. The NPs used in this study are nearly spherical in powder form, with an average size of 20 μm and 7 nm for NG and SiO_2 , respectively. Dispersion of the NPs and their static stability in the oil over time is ensured based on the dispersion test. A volumetric sample is taken from each blend and examined after each hour by the naked eye for any visible sedimentation. No sedimentations were observed during the first day of sample preparation; therefore, all the tribological tests were performed on the same day as the sample preparation, which was accomplished through the signification process. Multigrade oil was used to create the NP-based blends, and the viscosity of such oils is highly dependent on the temperature. The actual temperature of the interface may vary significantly depending on the lubrication domain being experienced by the interface. This oil temperature variation is in comparison with the ambient temperature and the bulk oil temperature in the sump. Therefore, conducting a comparative analysis for variations in oil viscosities because of NP concentration requires an in-depth study considering the

lubrication condition in the actual tribo-pair and is hence deliberately not presented here. This is a limitation of the present study, which will be addressed in the future.

Table 2. List of parameters involved and their values for the conducted experiments with multiple NPs.

Parameters	Minimum	Maximum	Average
SiO ₂ NP concentration (wt%)	0.2	0.4	0.3
NG NP concentration (wt%)	0.2	0.4	0.3
Load (N)	30	50	40
Speed (RPM)	35	100	58
Coefficient of friction	0.02	0.3	0.16

3. Computational Models of Lubricants

The initial study to develop the computational models of NP-based lubricants was initiated by training the RFT- and SVM-based regression models. The shortcomings of these two models directed the study to create more comprehensive ANN-based regression models to cater for the non-linearity involved in the experimental data of the lubricants. Developing the ANN-based computational model for hybrid nano lubricants with optimized parameters is daunting. It is required to capture the true behavior of the lubricant's tribology, as evident from the experimental data. This study employs the Bayesian optimization (BO) method to find optimal hyperparameters for the ANN models of NP-based lubricants. Once optimized hyperparameters are known, the ANN regression models are developed accordingly to estimate the CoF for the individual- and multiple-NP-based lubricants.

3.1. Training Dataset Generation

Multiple training datasets were developed from the experimental data to train the regression models. Two datasets contained the NP concentration, load, and speed as inputs along with the response variable CoF for both the NPs, i.e., SiO₂ and NG. The third dataset contained multiple NP concentrations as input along with the other parameters. All the inputs were rescaled with min–max normalization to regularize the data for loss function and to achieve rapid convergence during training. Input normalization was applied using the *normalize* built-in function of MATLAB 9.12 (MathWorks, Natick, MA, USA) according to the following relationship:

$$X'_i = a + \frac{X_i - \min(X_i)}{\max(X_i) - \min(X_i)}(b - a) \quad (1)$$

where X'_i is the normalized value and X_i is the original value of the input i , a and b are the normalization range limits which are set as $[a \ b] = [0 \ 1]$ for all the inputs.

3.2. Random Forest Trees

The initial regression model is developed using the ensemble method with bootstrap aggregating (bagging) of multiple decision trees (DT)-based regression learners. The random forest is developed at each ensemble split with a minimum leaf size of eight. A total of 30 DT learners were bagged in the ensemble with 100 learning cycles. The objective function is the MSE, which is minimized, and a threshold is set as a stopping criterion. The RFT training performance is evaluated via various regression performance assessment metrics such as root mean square error (RMSE), MSE, mean absolute error (MAE), and coefficient of determination (R-squared or R^2). All the training sessions are conducted using the 10-fold cross-validation, and the assessment metrics are calculated upon the validation results. The RFT model is implemented using the *fitensemble* built-in function of MATLAB 9.12.

3.3. Support Vector Machines

The other initial regression model is the non-linear SVM regression learner with a radial basis function (RBF) kernel for more accurate predictions. The rapid variations in the CoF are well predicted with the fine Gaussian SVM as compared with the polynomial-based SVM models. The fine Gaussian SVM employed a Gaussian kernel RBF with the kernel scale set to $\frac{\sqrt{P}}{4}$ for P number of predictors. For three input parameters of the individual NP-based datasets, the kernel scale is set to 0.43. In model designing, the box constraint and epsilon values are calculated heuristically by gradually increasing and decreasing them. Both these parameters are fine-tuned to generate a flexible model that avoids overfitting the predictions. The 10-fold cross-validation-based model training is conducted to achieve the best RMSE, MSE, MAE, and R^2 metrics results. The SVM regression model is implemented using the *fitrsvm* function of MATLAB 9.12.

3.4. Hyperparameter Estimation with Bayesian Optimization

The well-tuned hyperparameters for all the ANN models are computed with the BO algorithm, a derivative-free optimization method for non-analytical models. The MSE is used as the objective function $f(x)$, which is minimized upon subsequent iterations of the BO with different random samples of x according to the following relationship:

$$\min_{x \in A} f(x) = \min_{x \in A} (\text{MSE}) = \min_{x \in A} \left(\frac{1}{N} \sum_{i=1}^N (T_i - O_i)^2 \right)_{x \in \mathbb{R}^6} \quad (2)$$

where T_i and O_i are the actual target and predicted output values, respectively, for training sample i ranging from 1 to N number of observations, x is a random sample of six optimization variables for each iteration of the BO algorithm and always selected from the bounded domain of the structure A , containing search ranges for all the optimization variables as stated in Table 3.

Table 3. Optimized hypermeters and their search range for Bayesian optimization.

Optimization Variable (Hyperparameter)	Search Range for Optimization
Number of hidden layers	[1 3]
Number of neurons in 1st, 2nd, 3rd hidden layers	[1 300] for each layer
L2 Regularization strength (λ)	[1×10^{-6} 1×10^4]
Activation function	[ReLU Sigmoid Tanh None]

The selection of x from A for each iteration of BO is based upon the Gaussian distribution model, which is updated after each iteration to sample the x from the region that maximizes the acquisition function. The acquisition function (expected improvement per second plus) is used here, which is best for the global minimization of the objective function by avoiding the local minima. The local minima are avoided by the balanced exploration ratio of 0.5, which means an equal trade-off between the exploitation of already explored regions and the exploration of comparatively unexplored regions of A for sampling the new x . The maximization of the acquisition function, and hence, the convergence of the BO algorithm, is obtained by an iterative quasi-Newton numerical optimizer known as the limited-memory Broyden–Fletcher–Goldfarb–Shanno (LBFGS) algorithm. This way, the fine-tuned hyperparameters of x for global minimization of the MSE are computed using the BO method.

The additional hyperparameters are the data standardization and training iterations limit, which were not optimized and were set manually for multiple sessions of the BO algorithm for all the training datasets. As all the datasets were already normalized before the BO application, data standardization during the optimization process was set to false. All the sessions of BO were conducted with 10-fold cross-validation to find out the optimal and validated trained model. Ten sessions of the BO method were applied to each dataset

to ensure optimal hyperparameter tuning. After validation, the optimization results were selected for the session with the minimum RMSE, MSE, and MAE values and the maximum R^2 . The BO computational method is implemented using the *bayesopt* built-in function of MATLAB 9.12 and various optimization settings.

3.5. Design of Lubricant ANN Model

Once the optimized hyperparameters for all the lubricant models are computed, regression ANNs are developed from all three training datasets with fine-tuned hyperparameters. The general mathematical model for a single perceptron in all the ANNs is given below:

$$z_{j,i} = b_j + \sum_{i=1}^n w_{j,i} x_{j-1,i} \quad (3)$$

$$h_{j,i} = \sigma(z_{j,i}) = \frac{1}{1 + e^{-z_{j,i}}} \quad (4)$$

where $w_{j,i}$ is the weight for neuron i of the layer j , b_j is the bias term for a particular layer j , x is the input value from the preceding neuron, $z_{j,i}$ is the linear output value of all the connected weighted inputs subjected to the activation function, σ is the non-linear sigmoid activation function generating the final value $h_{j,i}$ for the neuron i in layer j .

Using the tuned hyperparameters, the regression ANN models are trained with different training algorithms for neural networks. The two variants of training algorithms were tested here for multiple training sessions, the scaled conjugate gradient (SCG) and the LM backpropagation from the conjugate gradient and the quasi-Newton families. These learning algorithms were implemented in MATLAB 9.12 with the built-in functions *trainscg* for SCG and *trainlm* for LM training methods. Among the various comparative runs for both methods, the SCG showed the best validation performance compared with LM for these smaller datasets. The SCG converged to a lower MSE with fewer iterations at the expense of training time. It also performed well during the testing of the approach with a varying number of hidden neurons, as it is less sensitive to hyperparameter changes than LM. The final design models of lubricant ANNs are generated with optimized hyperparameters and an SCG backpropagation learning scheme. The convergence information for all the ANNs, along with the hyperparameters, is shown in Table 4. The optimized number of hidden layers, hidden neurons, and their activation functions are obtained from the multi-session BO application on the datasets. To further validate the BO-based hyperparameter tuning results, trial tests were conducted by changing the numbers of hidden layers and hidden neurons. It was observed that further increasing the number of hidden layers and their sizes did not significantly improve the regression performance in terms of assessment metrics. Moreover, the prediction results of such trial models showed significant deviations from the experimental data. This ensured that the best hypermeter combination was selected by the BO, which reproduced the experimental results with high accuracy and precision. The best validation results of performance assessment metrics are obtained with these hyperparameters, as shown in Table 4.

Table 4. BO-estimated hyperparameters and convergence results for all lubricant ANN models.

ANN Model	Optimized Model Hyperparameters and Convergence Results							
	Hidden Layer Size	Activation Function	L2 Regularization ' λ '	Validation MSE at Epoch	Iterations	Training Loss	Gradient	Training Time (s)
SiO ₂ NP	10	sigmoid	0	7.81×10^{-4} at 37	43	52.31×10^{-4}	7.02×10^{-4}	213
NG NP	4	sigmoid	0	5.89×10^{-4} at 27	33	2.02×10^{-4}	10.01×10^{-4}	188
Multi-NP	2	sigmoid	0.11×10^{-4}	1.44×10^{-4} at 22	28	5.97×10^{-4}	3.96×10^{-4}	142

4. Results and Discussion

Figure 2 shows the regression plots for each NP with initial regression models, i.e., RFT and SVM. The best regression models with the most promising performance metrics are selected out of multiple training sessions with each regressor. The RFT regression plots show a significant sensitivity drift compared with the perfect predictions for both NPs, as shown in Figure 2a,b. The RFT prediction function follows the positive kurtosis with the leptokurtic distribution of predictions that can be observed from the regression plots. The RFT model failed to capture the complete variance of target data for the CoF predictions with 0.87 and 0.757 mean values for the coefficient of correlation (R) and R^2 , respectively. Moreover, a slight negative skewness of prediction distribution is observed towards higher target values of the CoF. On the other hand, the SVM regression model performed better with comparatively higher R and R^2 values, as shown in Figure 2c,d for SiO_2 and NG NPs, respectively. The sensitivity drift is significantly reduced as compared with the RFT, but few predicted values of the CoF still vary significantly from the target CoF. The kurtosis of prediction distribution is significantly reduced to mesokurtic in comparison with the leptokurtic distribution of the RFT model. These attributes and performance metrics results for both models are further compared with the final design of ANN-based regression models.

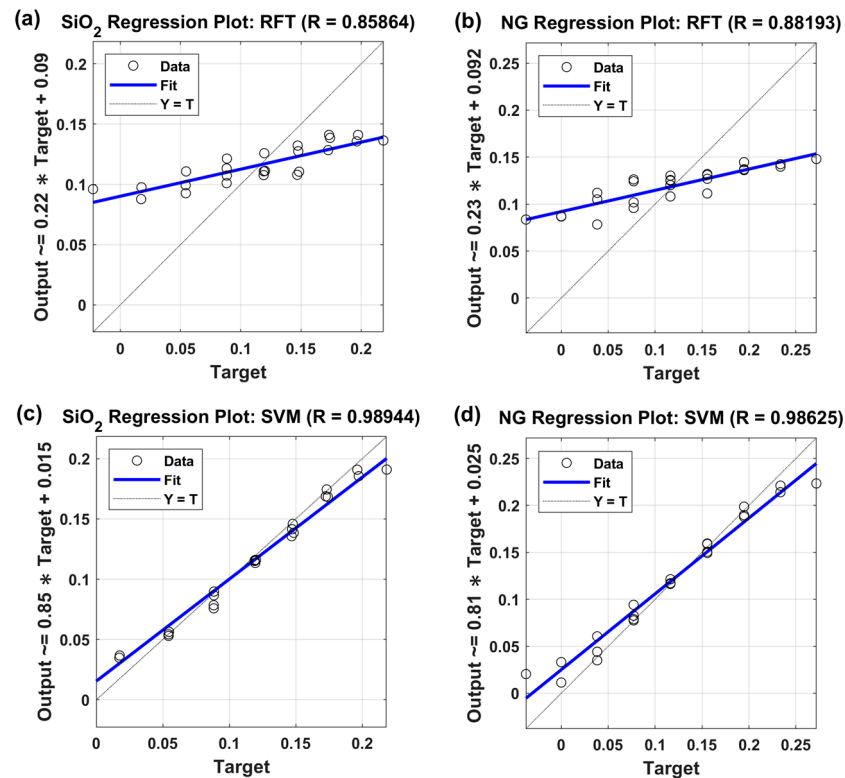


Figure 2. CoF computational efficiency for individual-NP-based lubricants with initial regression models (a) SiO_2 and (b) NG with RFT (c) SiO_2 and (d) NG with SVM.

The regression plots for the individual-NP-based and hybrid lubricant ANNs are shown in Figure 3. The regression plots for SiO_2 and NG ANN models in Figure 3a,b represent the best fit between the actual target values and ANN computed predictions of the CoF with higher R values.

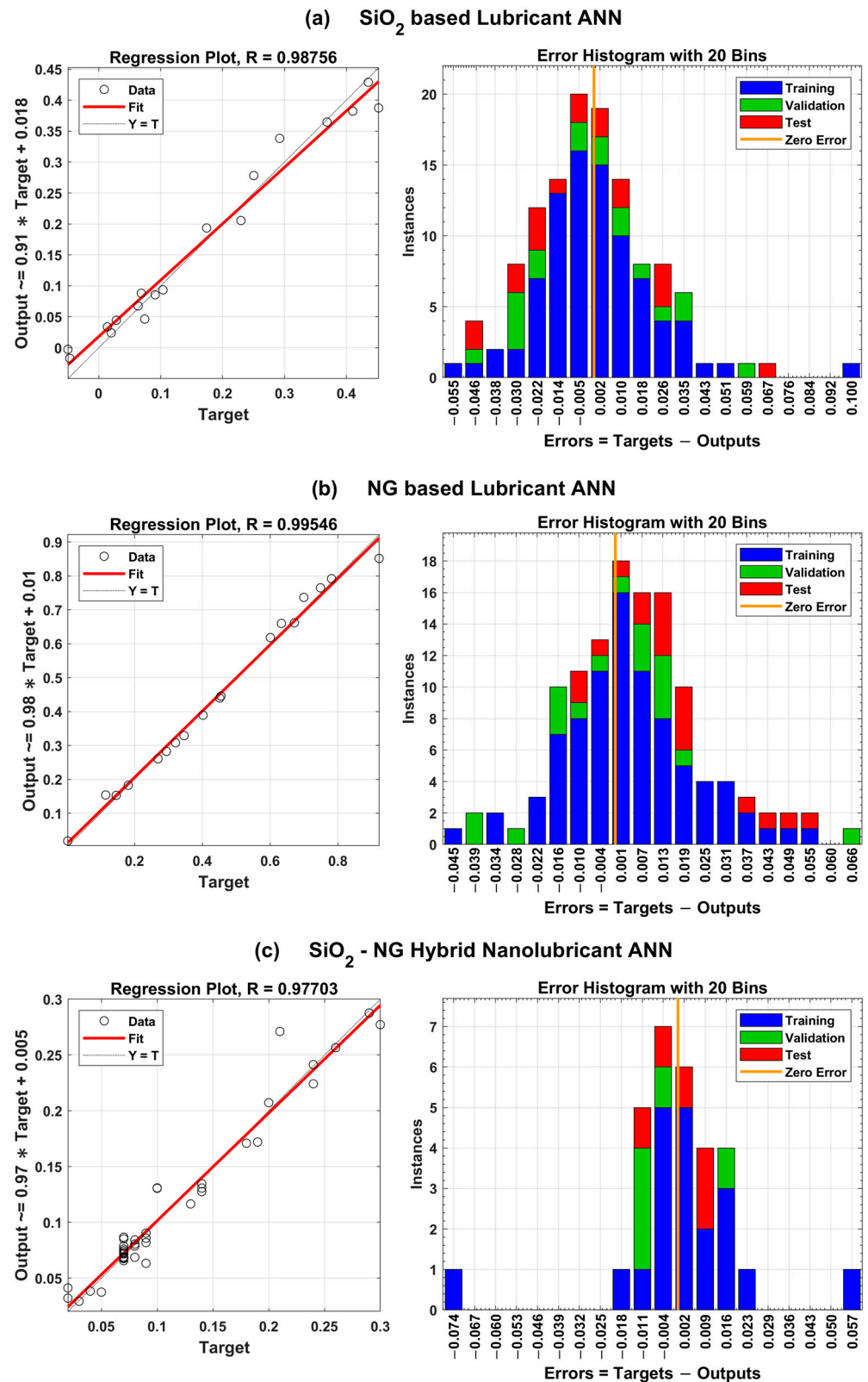


Figure 3. ANN models (regression plots, error histograms) for individual NP lubricants (a) SiO₂ (b) NG and (c) the multi-NP-based hybrid nano lubricant.

The R² is almost equal to one for all the models, representing the perfect estimation power of the designed ANNs and good confidence level in their computations. Moreover, these models are trained over a wide target range as compared with the initial models

and they performed better with comparatively good sensitivity over a larger spread of the target CoF. The error histograms show the perfect Gaussian distribution of training, testing, and validation errors during ANN model convergence.

These models can be further investigated to exhibit the behavior of NP-based lubricants in terms of the CoF, with varying input parameters such as NP concentration, load, and speed. Individual-NP-based lubricants mostly exhibit limitations in achieving the required tribological characteristics. To overcome these limitations, the hybrid nano lubricant ANN model is trained to achieve the benefits of both NPs to gain the required tribological properties of the lubricants. Figure 3c represents the regression plot along with the error histogram obtained during this ANN training. The regression plot with 0.9546 R^2 shows the good computational power of this model to find out the optimum CoF against the number of observations from the multi-NP-based training dataset. Few outlier samples in the regression plot achieved the training errors, with higher magnitudes on both sides of the zero error. Despite these countering outliers, the perfect regression fit is achieved. The rest of the error histogram shows that the ANN is well trained with the SCG method and has achieved minimal errors during the training, testing, and validation phases.

Table 5 shows the validation results of four regression performance assessment metrics, i.e., RMSE, R^2 , MSE, and MAE, for all the computational models (RFT, SVM, ANN) for both NPs and their hybrid (with ANN only). For SiO₂ NP, the ANN achieved the lowest RMSE, MSE, and MAE values with less difference from the SVM results and a significant difference from the RFT results. The R^2 for ANN and SVM is almost equal. For NG NP, SVM achieved slightly lower RMSE, MSE, and MAE values than the ANN, whereas the ANN achieved the best R^2 among all models.

Table 5. Performance assessment metrics results for all regression models with individual NP and hybrid nano lubricants.

Regression Model	Nanoparticle	Performance Assessment Metrics (10-Fold Cross-Validation)			
		RMSE	R^2	MSE	MAE
Random Forest Trees	SiO ₂	8.8662×10^{-3}	0.7373	7.8609×10^{-5}	7.9509×10^{-3}
	NG	6.7444×10^{-2}	0.7778	4.5487×10^{-3}	6.3266×10^{-2}
Support Vector Machines	SiO ₂	2.2689×10^{-3}	0.9790	5.1481×10^{-6}	2.1874×10^{-3}
	NG	3.2127×10^{-2}	0.9727	1.0321×10^{-3}	1.8183×10^{-2}
Artificial Neural Network	SiO ₂	2.2181×10^{-3}	0.9753	4.9199×10^{-6}	2.1026×10^{-3}
	NG	4.2407×10^{-2}	0.9909	1.7983×10^{-3}	3.1608×10^{-2}
	Hybrid	3.6296×10^{-2}	0.9546	1.3174×10^{-3}	2.3902×10^{-2}

Hence, these ANN models can be further investigated to study the tribological behavior of computationally designed lubricants that are influenced by the individual characteristics of multiple NPs. The inherent properties of such lubricant models can be utilized to achieve better CoF values with varying NP concentrations, load, and speed trends.

During the investigation of lubricant characteristics, it was observed that the speed is a less significant input as compared with the NP concentration and load. Substantial changes in the operating speed do not considerably affect the CoF for any load and concentration, whereas changing the NP concentration significantly affects the CoF of the lubricant. Figure 4 represents the characteristics of individual-NP-based lubricants with varying speeds and concentrations at a fixed load of 50 N. In an agreement with Bhaumik et al.'s study [29], it is evident that varying the concentration (with identical speeds) varies the CoF significantly. Thus, varying loading conditions results in variation in the optimum concentration to achieve CoF minima.

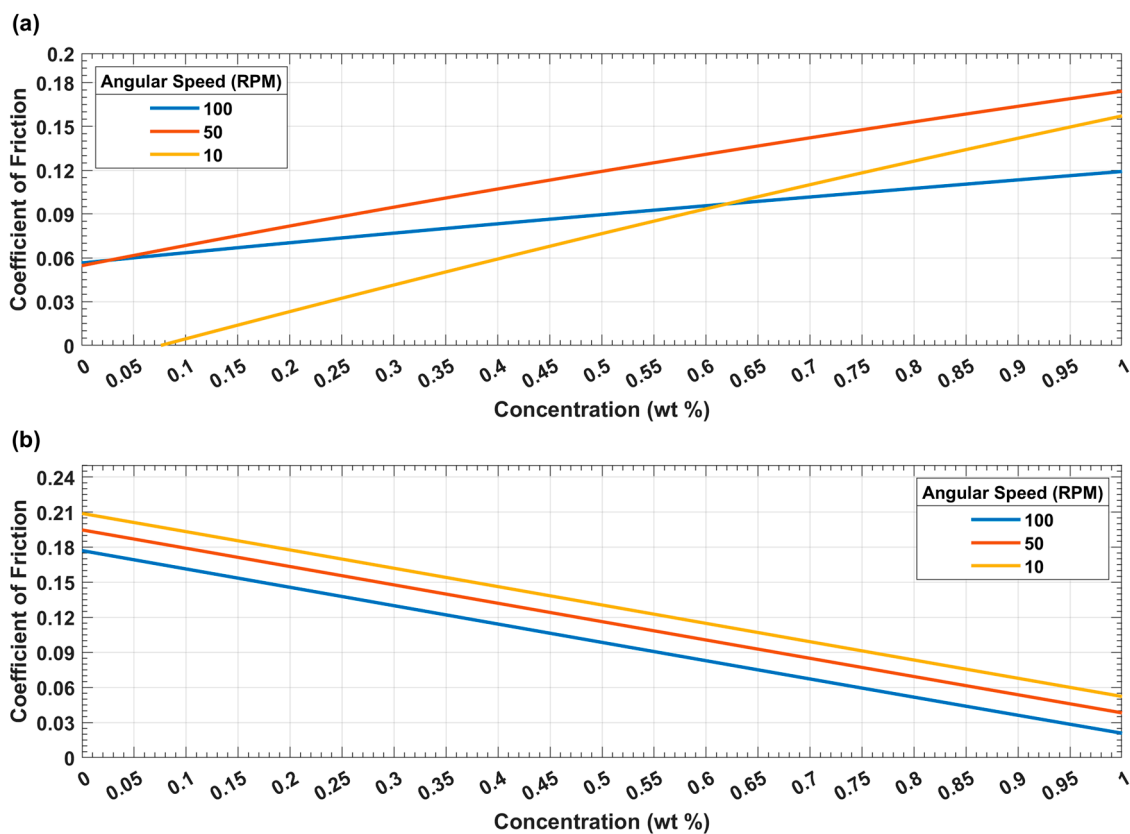


Figure 4. Significance of speed and NP concentration inputs to predict the CoF at a fixed load (50 N) for (a) SiO₂ and (b) NG nanoparticles.

Surface plots are developed to incorporate the influence of input parameters on the performance of the lubricants. Figure 5 represents the load–speed effects on the CoF with NP concentrations obtained for the individual-NP-based lubricants. These surfaces indicate that the load and NP concentrations are the influential input parameters in the NP-based lubricants and can drastically affect their tribological properties, as evident from the varying CoFs.

In Figure 5, the CoF has been plotted for varying loads and speeds for both NPs, i.e., SiO₂ and NG. Notably, regardless of the same base oil, the lubricating regimes vary for different NPs for the same loading conditions. An increasing and then decreasing CoF with increasing speeds for SiO₂ occurs, in contrast with NG, where the CoF decreases for growing speeds. This is attributed to the already fully developed lubricant oil film for the former one for identical loading conditions against the interface still experiencing mixed lubrication for the latter one. The decreasing CoF also highlights a thicker lubricant film with an increasing load because of shearing thinning for NG.

Moreover, a precise offset is evident in friction reduction with increasing concentration, regardless of the loading conditions. The percentage of each NP is different in oil to achieve an identical CoF, e.g., 1 wt% of SiO₂ and 0.1 wt% of NG results in a similar CoF at 100 RPM and counterbalance weight load conditions. This, and the above-mentioned existence of the interface in different lubricating regimes for identical loading conditions, makes it possible to develop a hybrid lubricant with more than one NP.

The magnitude of influence caused by a combination of NPs is illustrated in Figure 6 for identical speeds but at varying loads, i.e., 10–100 N. This is to observe the effect of NP combinations in different lubrication domains and how it influences the optimum concentration of the NPs to develop a composite N-enriched lubricant oil. NG facilitates the interface to reduce friction at low loads when the lubrication film thickness is well developed and the interface is experiencing pure hydrodynamic lubrication at a 10 N

load, as shown in Figure 6c. In contrast, when the load is increased, e.g., 50 N, as shown in Figure 6b, the local minima for the CoF move toward a high concentration for both the NPs and keep moving until they reach an equal concentration near (1,1). Similarly, with another increase in load, e.g., at 100 N, as in Figure 6a, the SiO₂ tends to facilitate the decrease in friction more compared with the NG. This could be because of the high molecular weight of SiO₂, which increases the viscosity more than NG, or better tribofilm development caused by SiO₂. The mechanism of friction reduction, and hence the different optimum concentrations at varying lubrication domains, is a limitation of the present work and will be reported on in a future publication.

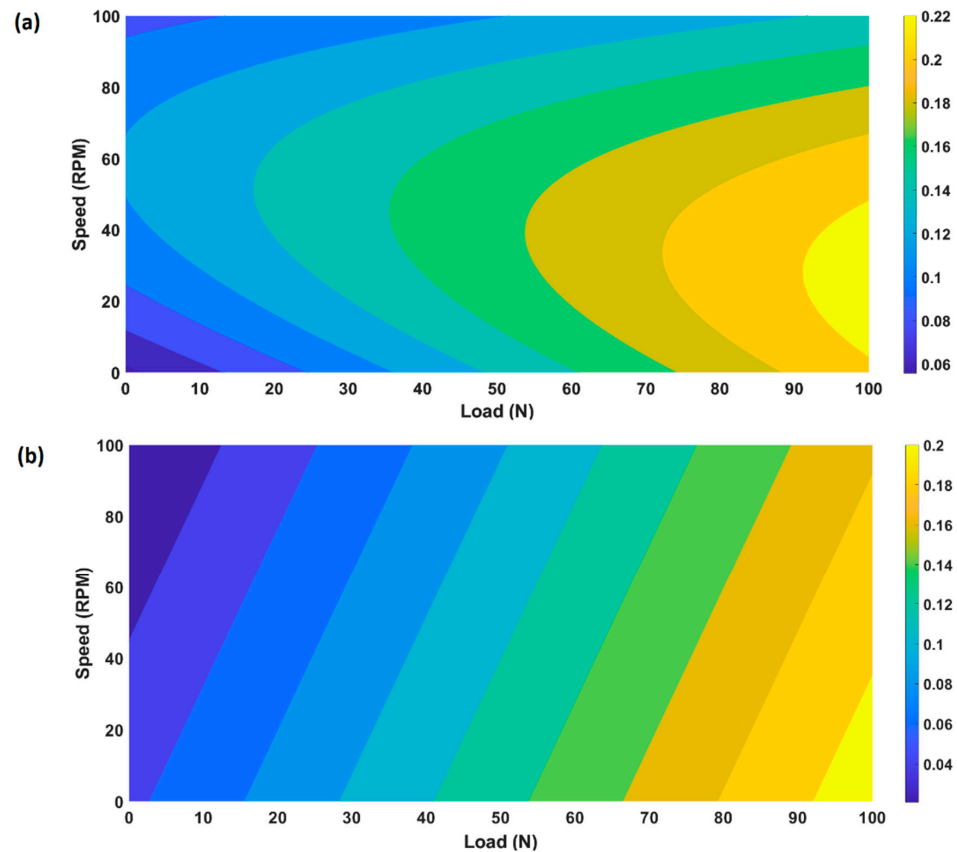


Figure 5. Speed and load effects on CoF for (a) SiO₂ with 1% concentration and (b) NG with 0.5% concentration.

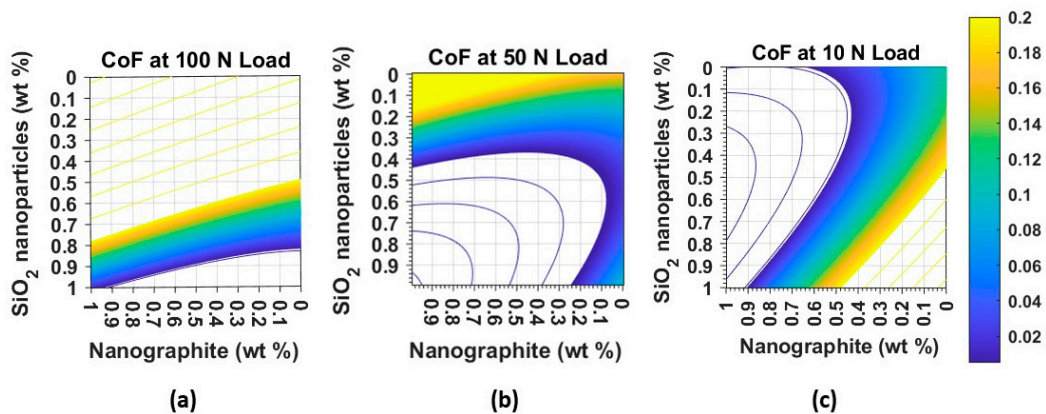


Figure 6. CoF estimation with hybrid-nano-lubricant-enriched lubricant oil containing ceramic and carbon-based NPs against varying concentrations at a constant speed (50 RPM) and three different loads; (a) 100 N, (b) 50 N, and (c) 10 N.

5. Conclusions

The coefficient of friction (CoF) in nano lubricants has a complex and non-linear relationship with its composition and loading conditions. Therefore, analytical models for predicting the tribological behavior of such lubricants are not available. A study is conducted utilizing machine learning (ML), and the following conclusions can be made from the observations of this study.

- The computational models given by the data-driven ML-based approaches such as random forest trees (RFT), support vector machines (SVM), and artificial neural networks (ANN) are promising solutions to predict non-linearity in such complex interactions.
- The multi-layered ANN-based regression models of lubricants having single and multiple nanoparticles (NP) are developed to examine their tribological behavior. The complex interactions of input parameters (load, speed, and NP concentration) and the output parameter (CoF) is well estimated by the ANNs when their hyperparameters are optimized.
- A better performance for ML-optimized nano lubricant models is found in decreasing the CoF between metal-to-metal interactions in sliding lubricated contact for engineering applications.
- The results have shown that the optimum concentration of NP varies with varying lubrication domains and that a composite lubricant based on multiple NPs can be beneficial to reduce frictional energy loss and improve the lubrication conditions.
- The optimum concentration of multiple NPs can be reached for interfaces that experience fluctuating loads and thus varying lubrication conditions during their service.

The future scope of this study is to examine the mechanism of friction reduction in hybrid nano lubricants with different NPs and base oil combinations. Finding out the optimum NP concentrations at varying lubrication domains is an underexplored research area requiring the further study of such ML-based applications.

Author Contributions: Conceptualization, A.U.; methodology, A.U. and S.A.; software, A.U. and S.A.; validation, A.U. and S.A.; formal analysis, A.U., S.A., M.L. and A.A.; investigation, A.U., S.A. and A.H.R.; resources, M.L. and A.A.; data curation, A.U. and A.H.R.; writing—original draft preparation, A.U. and S.A.; writing—review and editing, A.U., S.A., R.K., M.L. and A.A.; visualization, A.U., S.A. and A.H.R.; supervision, M.L. and A.A.; project administration, M.L. and A.A.; funding acquisition, M.L. and A.A. All authors have read and agreed to the published version of the manuscript.

Funding: This research was funded by the Swedish Research Council (VR) grant number 2019-04293.

Data Availability Statement: The data presented in this study are available on request from the corresponding author.

Acknowledgments: The authors acknowledge the technical and financial support provided by their organizations to complete this study.

Conflicts of Interest: The authors declare no conflict of interest.

References

1. Lim, S.C. Recent developments in wear-mechanism maps. *Tribol. Int.* **1998**, *31*, 87–97. [[CrossRef](#)]
2. Xiang, G.; Han, Y.; Wang, J.; Wang, J.; Ni, X. Coupling transient mixed lubrication and wear for journal bearing modeling. *Tribol. Int.* **2019**, *138*, 1–15. [[CrossRef](#)]
3. Xie, Z.; Jiao, J.; Yang, K. Experimental and numerical study on the mixed lubrication performances of a new bearing. *Tribol. Int.* **2023**, *182*, 108334. [[CrossRef](#)]
4. Li, W.; Wang, M.; Chen, Q.; Zhang, W.; Luo, T. A New Preparation Method of Copper oxide/Aluminium oxide Nanocomposites with Enhanced Anti-friction Properties. *ES Mater. Manuf.* **2023**, *19*, 692.
5. Jaffar, S.S.; Baqer, I.A.; Soud, W.A. Effect of Bi₂O₃ Nanoparticles Addition to Lubricating Oil on the Dynamic Behavior of Rotor-Bearing Systems. *J. Vib. Eng. Technol.* **2022**, *10*, 2005–2017. [[CrossRef](#)]

6. Zhao, Z.; Ma, Y.; Wan, H.; Ye, Y.; Chen, L.; Zhou, H.; Chen, J. Preparation and tribological behaviors of polyamide-imide/polytetrafluoroethylene lubricating coatings reinforced by in-situ synthesized CeO₂ nanoparticles. *Polym. Test.* **2021**, *96*, 107100. [[CrossRef](#)]
7. Ali, M.K.A.; Xianjun, H. Exploring the lubrication mechanism of CeO₂ nanoparticles dispersed in engine oil by bis(2-ethylhexyl) phosphate as a novel antiwear additive. *Tribol. Int.* **2022**, *165*, 107321. [[CrossRef](#)]
8. Lei, X.; Zhang, Y.; Zhang, S.; Yang, G.; Zhang, C.; Zhang, P. Study on the mechanism of rapid formation of ultra-thick tribofilm by CeO₂ nano additive and ZDDP. *Friction* **2023**, *11*, 48–63. [[CrossRef](#)]
9. Ghosh, S.K.; Miller, C.; Perez, G.; Carlton, H.; Huitink, D.; Beckford, S.; Zou, M. Effect of Cu nanoparticles on the tribological performance of polydopamine + polytetrafluoroethylene coatings in oil-lubricated condition. *Appl. Surf. Sci.* **2021**, *565*, 150525. [[CrossRef](#)]
10. Abdel-Rehim, A.A.; Akl, S.; Elsoudy, S. Investigation of the Tribological Behavior of Mineral Lubricant Using Copper Oxide Nano Additives. *Lubricants* **2021**, *9*, 16. [[CrossRef](#)]
11. Okokpujie, I.P.; Tartibu, L.K.; Sinebe, J.E.; Adeoye, A.O.M.; Akinlabi, E.T. Comparative Study of Rheological Effects of Vegetable Oil-Lubricant, TiO₂, MWCNTs Nano-Lubricants, and Machining Parameters' Influence on Cutting Force for Sustainable Metal Cutting Process. *Lubricants* **2022**, *10*, 54. [[CrossRef](#)]
12. Taha-Tijerina, J.; Aviña, K.; Diabb, J.M. Tribological and Thermal Transport Performance of SiO₂-Based Natural Lubricants. *Lubricants* **2019**, *7*, 71. [[CrossRef](#)]
13. Cortes, V.; Ortega, J.A. Evaluating the Rheological and Tribological Behaviors of Coconut Oil Modified with Nanoparticles as Lubricant Additives. *Lubricants* **2019**, *7*, 76. [[CrossRef](#)]
14. Mirzaamiri, R.; Akbarzadeh, S.; Ziaei-Rad, S.; Shin, D.-G.; Kim, D.-E. Molecular dynamics simulation and experimental investigation of tribological behavior of nanodiamonds in aqueous suspensions. *Tribol. Int.* **2021**, *156*, 106838. [[CrossRef](#)]
15. Wu, L.; Zhong, Y.; Yuan, H.; Liang, H.; Wang, F.; Gu, L. Ultra-dispersive sulfonated graphene as water-based lubricant additives for enhancing tribological performance. *Tribol. Int.* **2022**, *174*, 107759. [[CrossRef](#)]
16. Xu, M.; Wang, X.; Wang, T.; Wang, Q.; Li, S. Ag nanoparticle decorated graphene for improving tribological properties of fabric/phenolic composites. *Tribol. Int.* **2022**, *176*, 107889. [[CrossRef](#)]
17. Wang, G.; Ruan, Y.; Wang, H.; Zhao, G.; Cao, X.; Li, X.; Ding, Q. Tribological performance study and prediction of copper coated by MoS₂ based on GBRT method. *Tribol. Int.* **2023**, *179*, 108149. [[CrossRef](#)]
18. Yu, Z.; Wang, S.; Cheng, J.; Chen, J.; Chen, W.; Sun, Q.; Yang, J. Tribological behaviors of MoAlB ceramic in artificial seawater. *Tribol. Int.* **2022**, *167*, 107345. [[CrossRef](#)]
19. Pham, S.T.; Huynh, K.K.; Tieu, K.A. Tribological performances of ceramic oxide nanoparticle additives in sodium borate melt under steel/steel sliding contacts at high temperatures. *Tribol. Int.* **2022**, *165*, 107296. [[CrossRef](#)]
20. Simonovic, K.; Vitu, T.; Cammarata, A.; Cavaleiro, A.; Polcar, T. Tribological behaviour of W-S-C coated ceramics in a vacuum environment. *Tribol. Int.* **2022**, *167*, 107375. [[CrossRef](#)]
21. Xu, Z.; Zhong, M.; Xu, W.; Xie, G.; Hu, H. Effects of aluminosilicate particles on tribological performance and friction mechanism of Cu-matrix pads for high-speed trains. *Tribol. Int.* **2023**, *177*, 107983. [[CrossRef](#)]
22. Chen, F.; Yan, K.; Hong, J.; Song, J. Synergistic effect of graphene and β-Si₃N₄ whisker enables Si₃N₄ ceramic composites to obtain ultra-low friction coefficient. *Tribol. Int.* **2023**, *178*, 108045. [[CrossRef](#)]
23. Fahad, M.R.; Abdulmajeed, B.A. Experimental investigation of base oil properties containing modified TiO₂/CuO nanoparticles additives. *J. Phys. Conf. Ser.* **2021**, *1973*, 012089. [[CrossRef](#)]
24. Sharma, A.K.; Tiwari, A.K.; Dixit, A.R.; Singh, R.K.; Singh, M. Novel uses of alumina/graphene hybrid nanoparticle additives for improved tribological properties of lubricant in turning operation. *Tribol. Int.* **2018**, *119*, 99–111. [[CrossRef](#)]
25. Huang, S.; He, A.; Yun, J.-H.; Xu, X.; Jiang, Z.; Jiao, S.; Huang, H. Synergistic tribological performance of a water based lubricant using graphene oxide and alumina hybrid nanoparticles as additives. *Tribol. Int.* **2019**, *135*, 170–180. [[CrossRef](#)]
26. de Oliveira, L.R.; Rodrigues, T.A.; Costa, H.L.; da Silva, W.M., Jr. Scuffing resistance of polyalphaolefin (PAO)-based nanolubricants with oleic acid (OA) and iron oxide nanoparticles. *Mater. Today Commun.* **2022**, *31*, 103837. [[CrossRef](#)]
27. Liñeira del Río, J.M.; López, E.R.; González Gómez, M.; Yáñez Vilar, S.; Piñeiro, Y.; Rivas, J.; Gonçalves, D.E.P.; Seabra, J.H.O.; Fernández, J. Tribological Behavior of Nanolubricants Based on Coated Magnetic Nanoparticles and Trimethylolpropane Trioleate Base Oil. *Nanomaterials* **2020**, *10*, 683. [[CrossRef](#)] [[PubMed](#)]
28. Alvi, M.A.A.; Belayneh, M.; Bandyopadhyay, S.; Minde, M.W. Effect of Iron Oxide Nanoparticles on the Properties of Water-Based Drilling Fluids. *Energies* **2020**, *13*, 6718. [[CrossRef](#)]
29. Bhaumik, S.; Pathak, S.D.; Dey, S.; Datta, S. Artificial intelligence based design of multiple friction modifiers dispersed castor oil and evaluating its tribological properties. *Tribol. Int.* **2019**, *140*, 105813. [[CrossRef](#)]
30. Humelnicu, C.; Ciortan, S.; Amortila, V. Artificial Neural Network-Based Analysis of the Tribological Behavior of Vegetable Oil–Diesel Fuel Mixtures. *Lubricants* **2019**, *7*, 32. [[CrossRef](#)]
31. Haldar, A.; Chatterjee, S.; Kotia, A.; Kumar, N.; Ghosh, S.K. Analysis of rheological properties of MWCNT/SiO₂ hydraulic oil nanolubricants using regression and artificial neural network. *Int. Commun. Heat Mass Transf.* **2020**, *116*, 104723. [[CrossRef](#)]
32. Esfe, M.H.; Toghraie, D.; Amoozadkhalili, F. Optimization and design of ANN with Levenberg-Marquardt algorithm to increase the accuracy in predicting the viscosity of SAE40 oil-based hybrid nano-lubricant. *Powder Technol.* **2023**, *415*, 118097. [[CrossRef](#)]

33. Sharma, G.; Kotia, A.; Ghosh, S.K.; Rana, P.S.; Bawa, S.; Ali, M.K.A. Kinematic viscosity prediction of nanolubricants employed in heavy earth moving machinery using machine learning techniques. *Int. J. Precis. Eng. Manuf.* **2020**, *21*, 1921–1932. [[CrossRef](#)]
34. Qing, H.; Hamed, S.; Eftekhari, S.A.; Alizadeh, S.M.; Toghraie, D.; Hekmatifar, M.; Ahmed, A.N.; Khan, A. A well-trained feed-forward perceptron Artificial Neural Network (ANN) for prediction the dynamic viscosity of Al₂O₃–MWCNT (40:60)-Oil SAE50 hybrid nano-lubricant at different volume fraction of nanoparticles, temperatures, and shear rates. *Int. Commun. Heat Mass Transf.* **2021**, *128*, 105624. [[CrossRef](#)]

Disclaimer/Publisher’s Note: The statements, opinions and data contained in all publications are solely those of the individual author(s) and contributor(s) and not of MDPI and/or the editor(s). MDPI and/or the editor(s) disclaim responsibility for any injury to people or property resulting from any ideas, methods, instructions or products referred to in the content.